Supplement of Atmos. Chem. Phys., 26, 4215–4230, 2026
https://doi.org/10.5194/acp-26-4215-2026-supplement


Atmospheric Chemistry and Physics
Open Access

*Supplement of*

# Size-resolved condensation sink as an approach to understand pathways how gaseous emissions affect health and climate

**Teemu Lepistö et al.**

*Correspondence to:* Teemu Lepistö (teemu.lepisto@tuni.fi)

## List of parameter definitions and utilised default values in the ELPI+ CS calibration

**Table S1: Parameters in the ELPI+ CS calibration**

| Parameter | Description | Value (by default) |
|---|---|---|
| *Pn* | ELPI+ charging efficiency (multiplication of *P,* the particle penetration through the charger, and *n,* the number of elementary charges carried by particles after charging | See Equation 1 |
| $d_p$ | Particle diameter, in this study, referred as the particle mobility equivalent diameter | |
| *e* | Elementary charge | $1.602176487*10^{-19}$ C |
| Q | Nominal sample flow of the ELPI+ | 10 lpm |
| $\rho_{eff}$ | Particle effective density | 1.0 $g/cm^3$ |
| $A_{CS}$ | Attachment rate factor of vapour molecules onto the particles | See Equation 2 |
| *D* | Diffusion constant for the considered vapour molecule (i.e. sulphuric acid) in air | See Equation 3 |
| $\beta$ | Fuchs-Sutugin correction factor | See Equation 4 |
| *T* | Ambient temperature | 20° C |
| $M_{air}$ | Molecular weight of air | 28.965 g/mol |
| $M_{vap}$ | Molecular weight of the considered vapour molecule, i.e. sulphuric acid | 98.08 g/mol |
| $D_{x,air}$ | Diffusion volume of air | 19.7 |
| $D_{x,vap}$ | Diffusion volume of the considered vapour molecule, i.e. sulphuric acid | 51.66 |
| Kn | Knudsen number | See Equation 5 |
| $\lambda_{vap}$ | Mean free path of the considered vapour molecule, i.e. sulphuric acid | See Equation 6 |
| $\alpha$ | Mass accommodation coefficient | 1.0 |
| $m_{vap}$ | Mass of a single vapour molecule, i.e. sulphuric acid | $1.6287*10^{-25}$ kg |
| $k_b$ | Boltzmann constant | $1.380649*10^{-23}$ J/K |
| *K* | Size dependent CS response function of ELPI+ | See Equation 7 |
| $dpMean_a$ | The geometric mean (aerodynamic) size of particles collected onto each impactor stage of the ELPI+ impactor. | |
| $d_a$ | Particle aerodynamic diameter | |
| $C_c$ | Cunningham slip correction factor | $1 + (66/d_p)*(2.34 + 1.05*exp(-0.39*d_p/66))$ ($d_p$ in nanometres) |

## ELPI+ CS response with varying input parameters

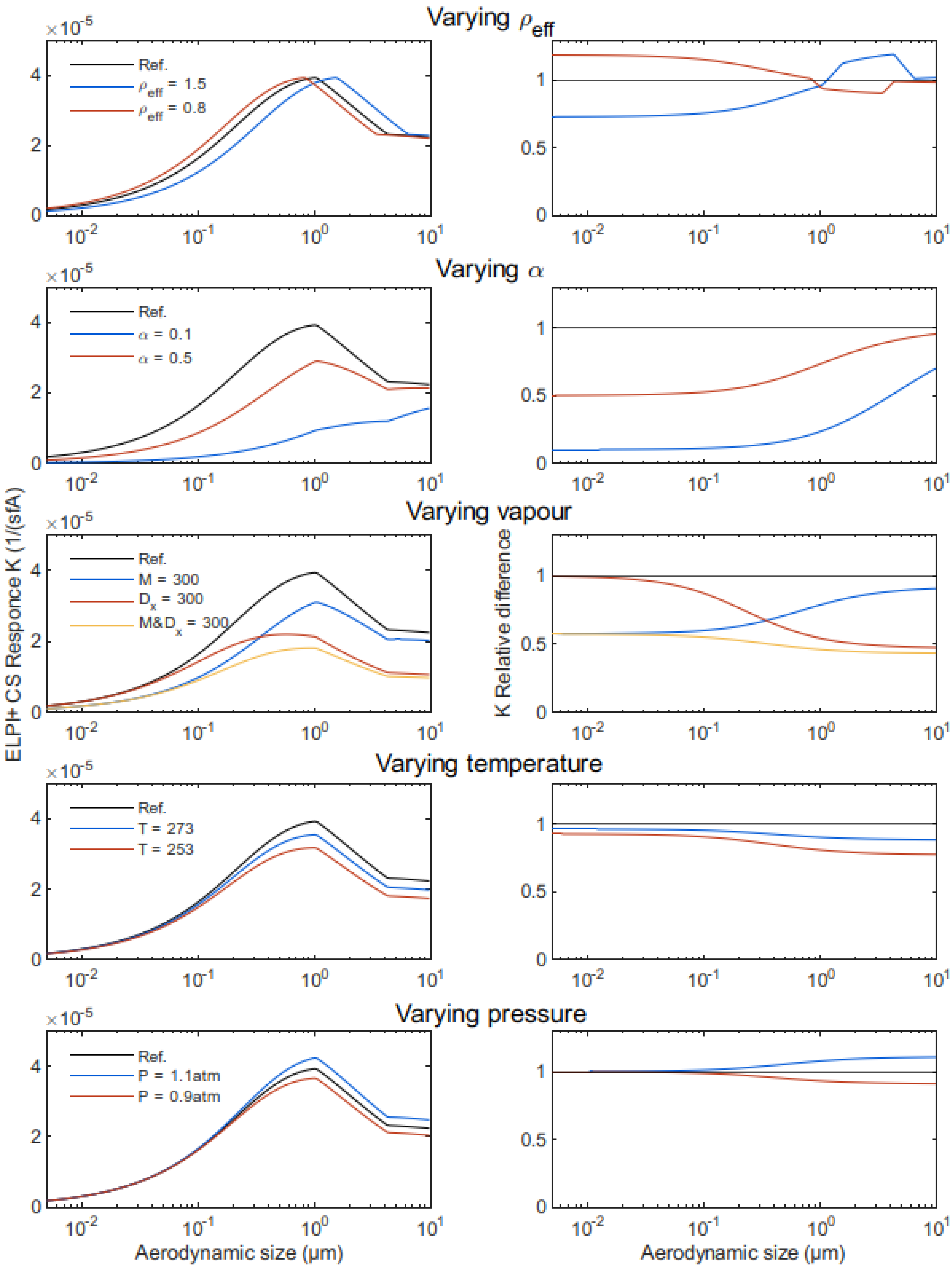


**Figure S1: The ELPI+ CS response coefficient (i.e. conversion factor) as a function of particle size with varying parameters related to particle effective density ($\rho_{eff}$, g/cm$^3$), accommodation coefficient (α), vapour molar mass (M, g/mol) and diffusion volume ($D_x$, cm$^3$), ambient temperature (T, K) and pressure (P). The reference values for $\rho_{eff}$, α, M, $D_x$, T and P are 1.0 g/cm$^3$, 1.0, 98.08 g/mol, 51.66 cm$^3$, 293.15 K and 1 atm.**

## The ELPI+ and DMPS comparison campaign

**Table S2: Average measured concentrations during different pollution episodes of the DMPS and ELPI+ comparison campaign in Helsinki.**

| | Helsinki: No episode | Helsinki: Inversion | Helsinki: LRT |
|---|---|---|---|
| **PN (1 $cm^{-3}$)** | 7 700 | 16 200 | 9 700 |
| **PM2.5 (µg $m^{-3}$)** | 3.4 | 9.9 | 15.4 |
| **NO (µg $m^{-3}$)** | 16.1 | 29.8 | 22.2 |
| **BC (µg $m^{-3}$)** | 0.58 | 1.11 | 1.01 |
| **$\rho_{eff}$ (g $cm^{-3}$)** | 1.1 | 1.3 | 1.7 |

## Description of the measurement campaigns

**Table S3: Description of the measurement campaigns and utilised data.**

| Campaign | Location | Description |
|---|---|---|
| **Helsinki, ELPI+ and DMPS comparison (01-02/2022)** | Urban traffic | The measurements were conducted on a kerbside in a street canyon, including 3+3 driving lanes. The DMPS measured in an air quality monitoring station, and the ELPI+ in a mobile laboratory right next to the station. The measurements were carried out daily between 06:30 and 19:30. The weather conditions were typical wintertime conditions in Helsinki. During the inversion episode, temperature was below −5 °C, reducing the dilution and dispersion of pollutants. During the LRT episode, air masses in Helsinki had travelled through Central and Eastern Europe. |
| **Helsinki, Summer (08/2019) (see [2])** | Urban traffic | The measurements carried out in the same street canyon as the ELPI+ and DMPS comparison. The measurement were conducted with a mobile laboratory. The utilised data was measured between 6 am and 6 pm. |
| | Highway | The measurement site was next to Länsiväylä highway in Espoo (Helsinki metropolitan area), approximately 20 meters from the road. The average weekday traffic on the highway was 70 000 vehicles in 2019. The measurement were conducted with a mobile laboratory. The utilised data was measured between 6 am and 6 pm. |
| | Shipping | The data was measured in the Harbour B location of the corresponding publication (Lepistö et al. 2022) in Helsinki. The measurement were conducted with a mobile laboratory. Harbour B location was relatively far away from other pollution sources like road traffic, and, therefore, it can be better considered to represent the emissions from the ships. During the measurements, dominating wind direction was from the sea (and harbour area) to the measurement location. |
| **Helsinki, Winter (03/2021) (see [3])** | Urban traffic | The measurements carried out in the same street canyon as the ELPI+ and DMPS comparison and Helsinki, Summer 2019. The measurement were conducted with a mobile laboratory. The utilised data is based on measurement on 2nd and 8th March when there was not a LRT-episode affecting the results. |

| | | |
|---|---|---|
| | Airport | The measurements were conducted with a mobile laboratory next to Helsinki-Vantaa airport, approximately 200 m away from the closest (and the most active) runway. Due to the SARS-CoV-2 outbreak, air traffic was significantly reduced during the campaign, and the measurements were targeted on times, when the wind was from the airport, and the airport activity was high (take-offs approximately every 5 min). |
| | Residential area | The measurements were conducted with a mobile laboratory in a detached-housing residential area in Vantaa (Helsinki metropolitan area). The utilised data was measured during the evening when the effects of residential wood combustion was the clearest (cold Friday evening, March 5th). |
| **Tampere (04-05 2020)** | Highway | The measurements were conducted by driving the mobile laboratory back-and-forth an busy arterial road and a motorway. The utilised data was measured between 6 am and 6 pm. |
| **Raahe (01-02/2021) (see [1])** | Residential area | The data was measured with a mobile laboratory in detached-housing residential area. Only evening data considered as the effects of residential wood combustion were the clearest during the evenings. Only the data measured when the wind was not from the nearby steel factory considered. |
| | Industrial | The data was measured with a mobile laboratory in an background site when the wind was from the nearby steel factory (approximately 2 km away from the factory). |
| **Düsseldorf (03/2022)** | Urban traffic | The measurement site located next to an arterial road in a low emission zone, allowing only the use of vehicles that fulfil EURO 4 emission standard. The measurement were conducted with a mobile laboratory. The utilised data was measured between 6 am and 6 pm. |
| | Highway | The measurements were done by driving on motorways near Düsseldorf airport. The utilised data was measured between 6 am and 6 pm. |
| | Airport | The measurements were done in a residential area near Düsseldorf airport (2 – 3 km away). Only the data measured when the wind was from the airport were considered. |
| | Riverside | The measurements were done in a residential area right next to river Rhine (50 – 300 m away from the passing ships). Only the data measured when the wind was blowing from the river were considered. |
| **Prague (03-04/2022)** | Urban traffic | The site located in a preschool yard next to a two-lane street having two tramlines in the middle. The measurements were carried out with a mobile laboratory. The utilised data was measured between 6 am and 6 pm. |
| | Highway | The measurements were done with a mobile laboratory right next to a busy six-lane arterial road in-and-out the city. The utilised data was measured between 6 am and 6 pm. |
| **Delhi-NCR (11-12/2018) (see [4])** | Urban traffic | The measurement site was along a busy road with two lanes in both directions. The ambient temperature varied between 8 °C to 20 °C during the period. All the data reported by Salo et al. (2021) were utilised. |

[1] Barreira, et al. (2023). Comprehensive characterization of wintertime submicron aerosol in a Nordic town influenced by residential wood combustion, traffic and industrial sources. Atmospheric Pollution Research, 14, 8. DOI: 10.1016/j.apr.2023.101835

[2] Lepistö, et al. (2022). Connection between lung deposited surface area (LDSA) and black carbon (BC) concentrations in road traffic and harbour environments. Atmospheric Environment, 272. DOI: 10.1016/j.atmosenv.2021.118931.

[3] Lepistö, et al. (2023). Snapshots of wintertime urban aerosol characteristics: Local sources emphasized in ultrafine particle number and lung deposited surface area, Environmental Research, 231, 1. DOI: 10.1016/j.envres.2023.116068.

[4] Salo, L., et al. (2021). The characteristics and size of lung-depositing particles vary significantly between high and low pollution traffic environments. Atmospheric Environment 255, 118421. https://doi.org/10.1016/j.atmosenv.2021.118421

## The size distributions results of the simulations

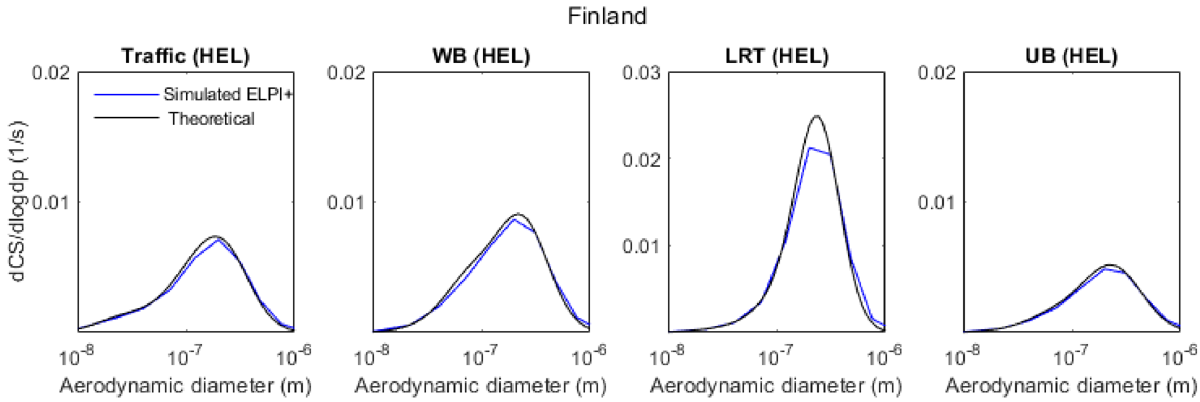


**Figure S2: The simulated and theoretical CS size distributions based on the size distributions reported from Finland (Table 2). WB = Wood burning, LRT = long-range transported, UB = Urban background.**

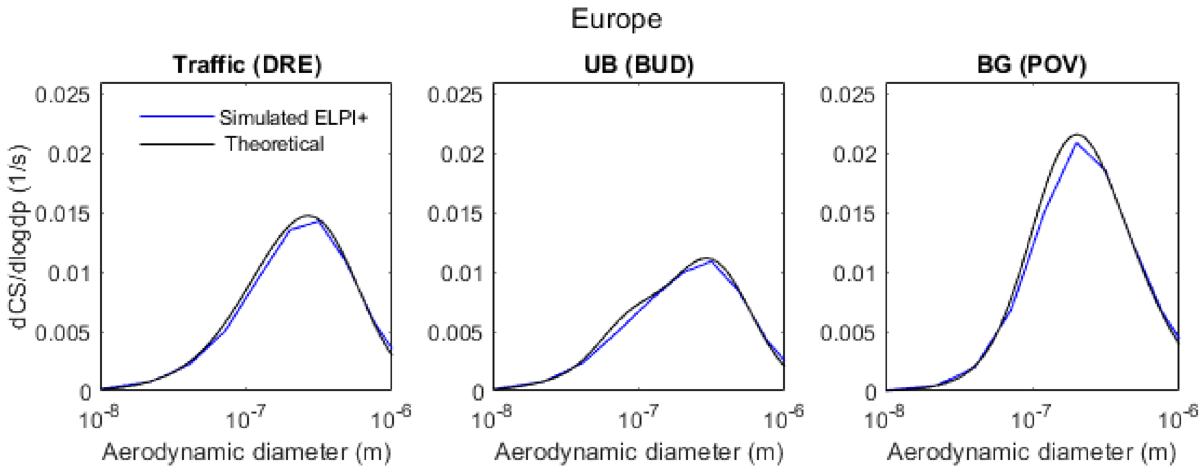


**Figure S3: The simulated and theoretical CS size distributions based on the size distributions reported from Europe (Table 2). UB = Urban background, BG = Background, DRE = Dresden, BUD = Budapest, POV = Po Valley.**

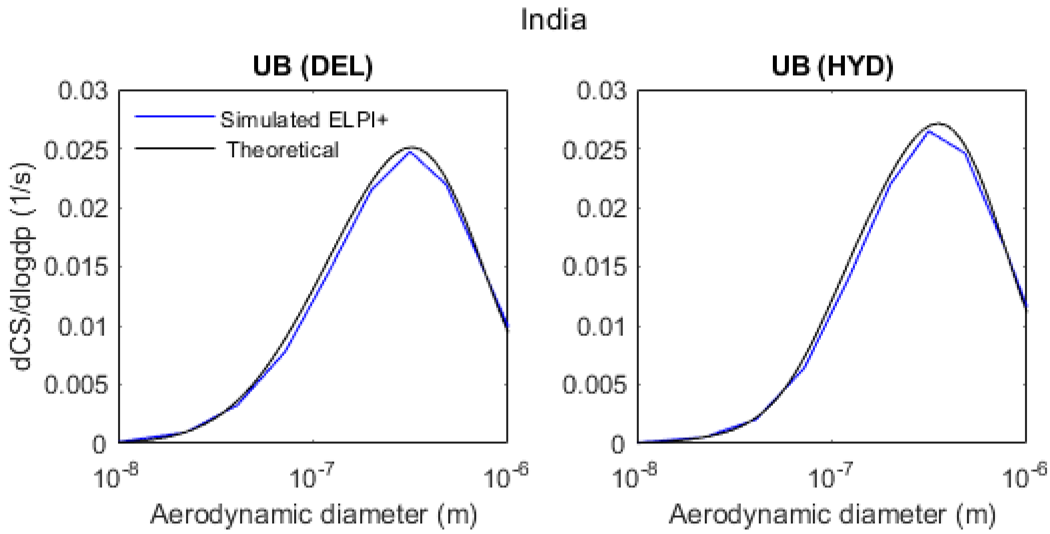


**Figure S4: The simulated and theoretical CS size distributions based on the size distributions reported from India (Table 2). UB = Urban background, DEL = Delhi, HYD = Hyderabad.**

**The measured CS with different assumed particle effective densities**

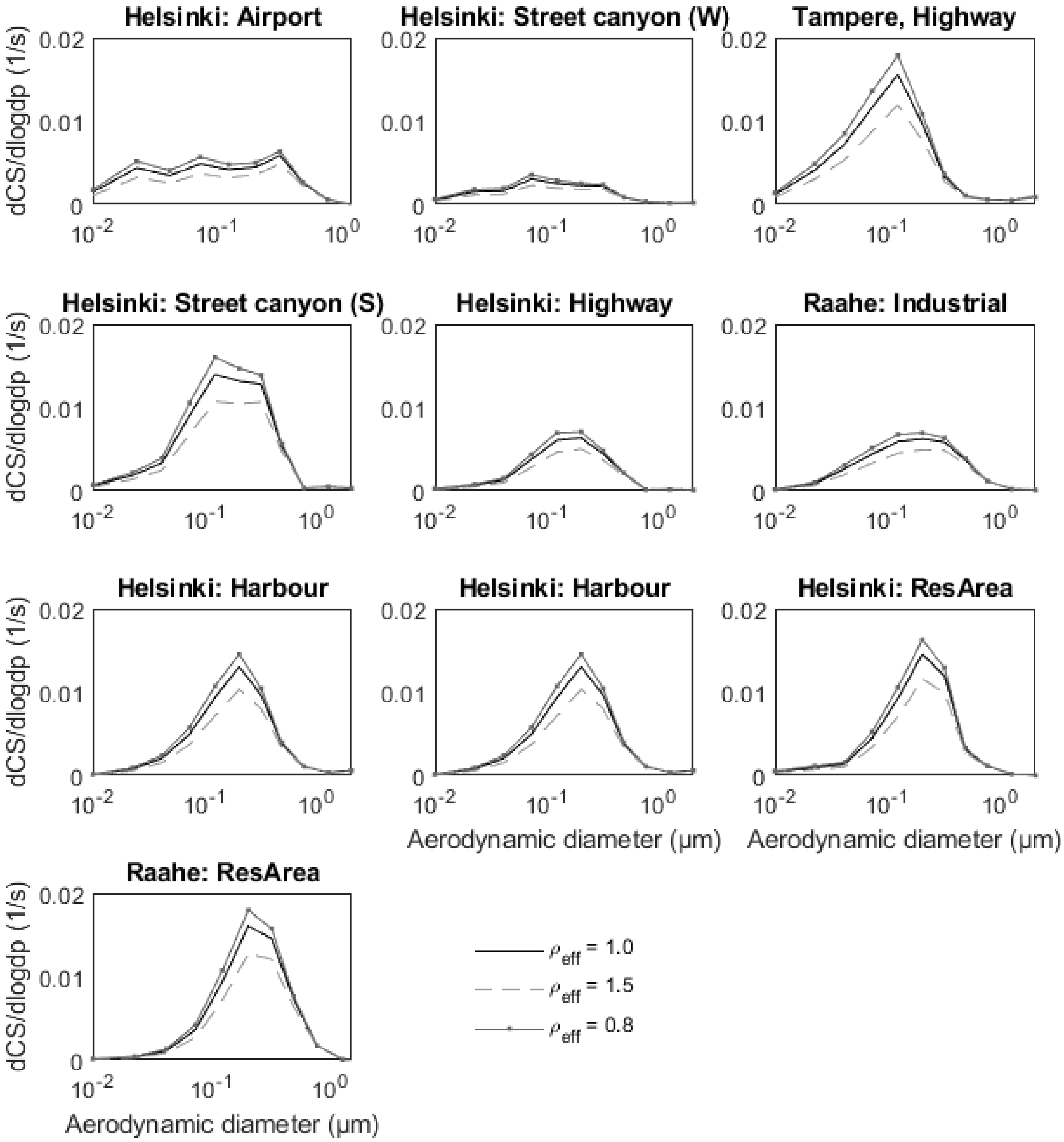


**Figure S5: Average CS size distributions measured in Finland with assumed effective densities of 1.0, 1.5 and 0.8 g/cm$^3$.**

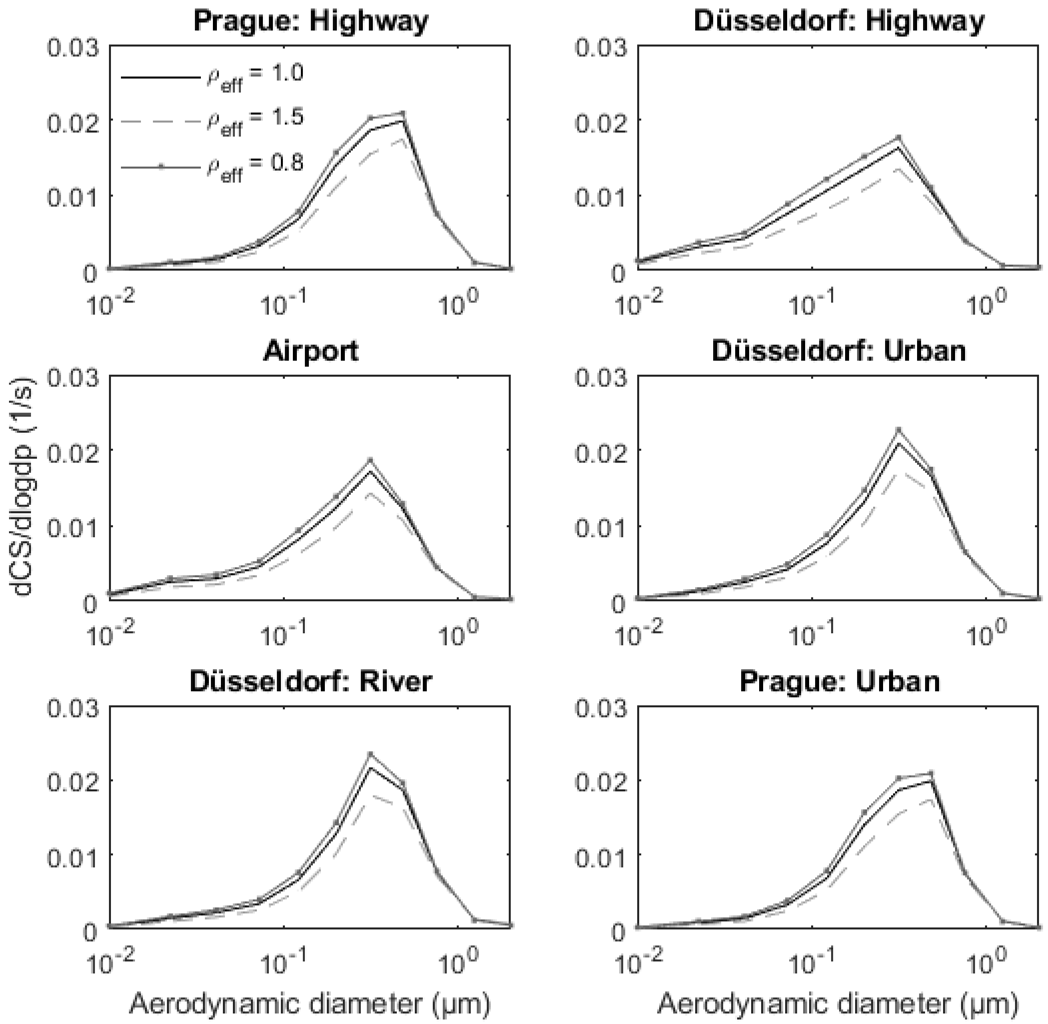


**Figure S6: Average CS size distributions measured in Central Europe with assumed effective densities of 1.0, 1.5 and 0.8 g/cm$^3$.**

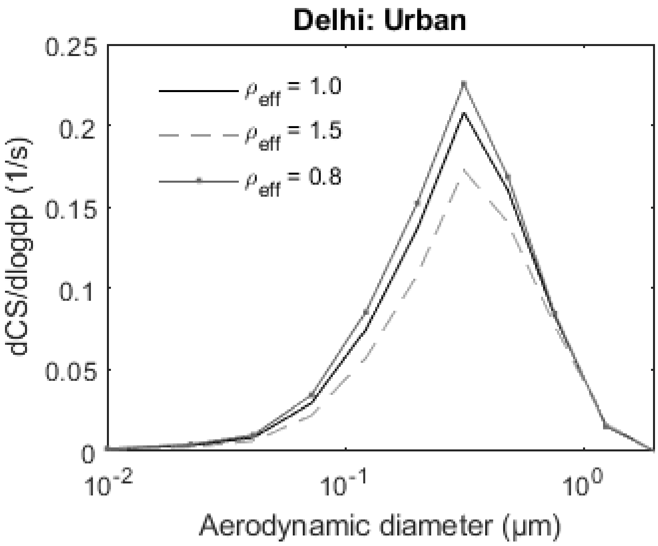


**Figure S7: Average CS size distribution measured in Delhi-NCR with assumed effective densities of 1.0, 1.5 and 0.8 g/cm$^3$.**

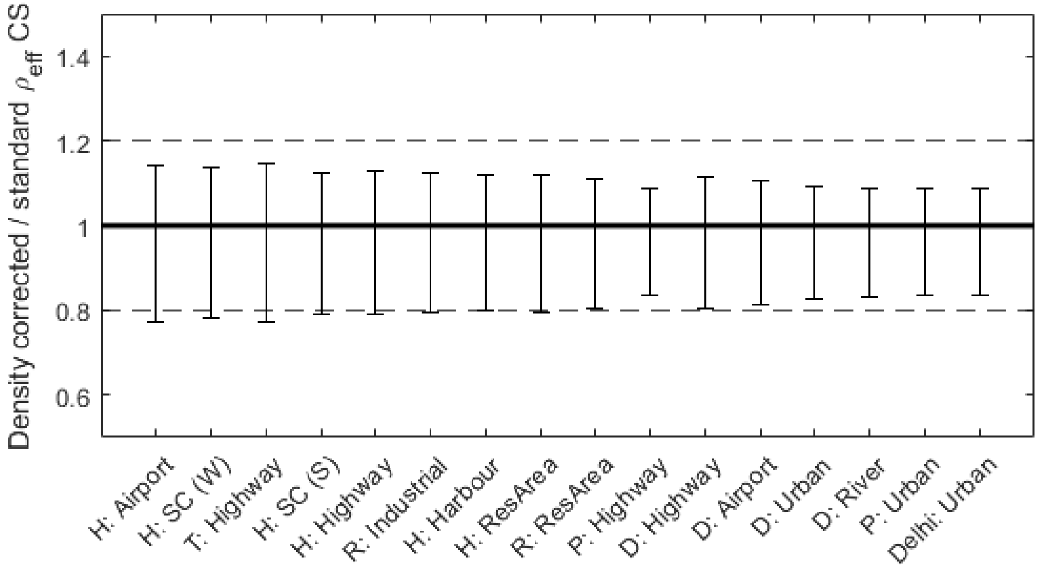


**Figure S8: The density corrected ELPI+ CS (with $\rho_{eff}$ 0.8–1.5 g/cm$^3$) compared to the standard $\rho_{eff}$ assumed measurement.**

**The measured CS with different input parameters**

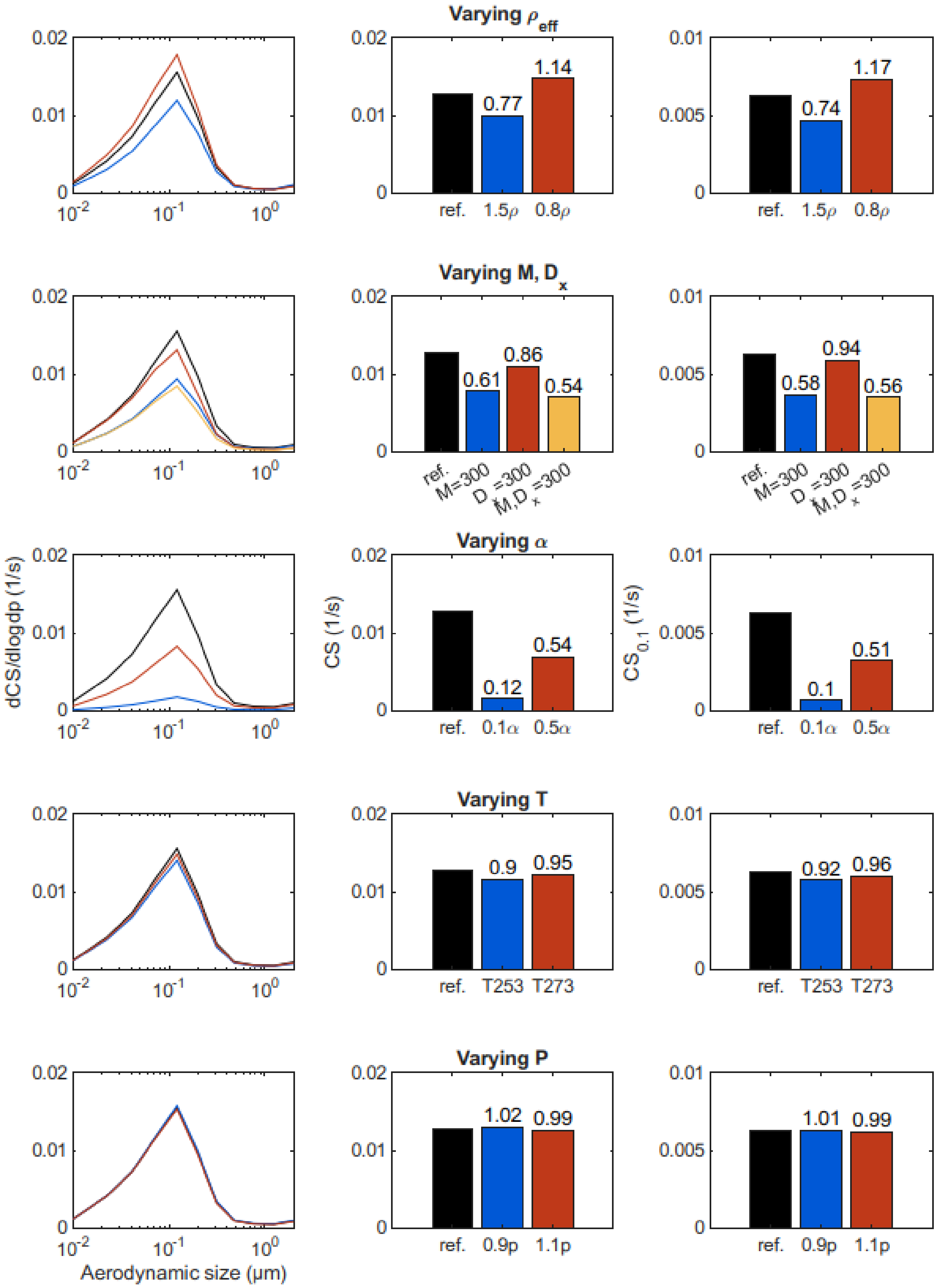


**Figure S9: The effect of varying input parameters of the calculation ($\rho_{eff}$, $\alpha$, $M_{vap}$, $D_{x,vap}$, $T$, $P$) on CS, $CS_{0.1}$ and CS size distribution at the studied location of Highway (Tampere). 1.5$\rho$ and 0.8$\rho$ indicate $\rho_{eff}$ of 1.5 and 0.8 g/cm$^3$, respectively. M = 300, $D_x$ = 300 indicate $M_{vap}$ of 300 g/mol, $D_{x,vap}$ of 300 cm$^3$, respectively (M,$D_x$ = 300 indicates both). 0.1$\alpha$ and 0.5$\alpha$ indicate $\alpha$ of 0.1 and 0.5, respectively. T253, T273, 0.9p and 1.1p indicate temperatures of 253 K and 273 K, and ambient pressure of 0.9 atm and 1.1 atm. The value on the bar plot shows the difference to default input parameter values (ref.)**

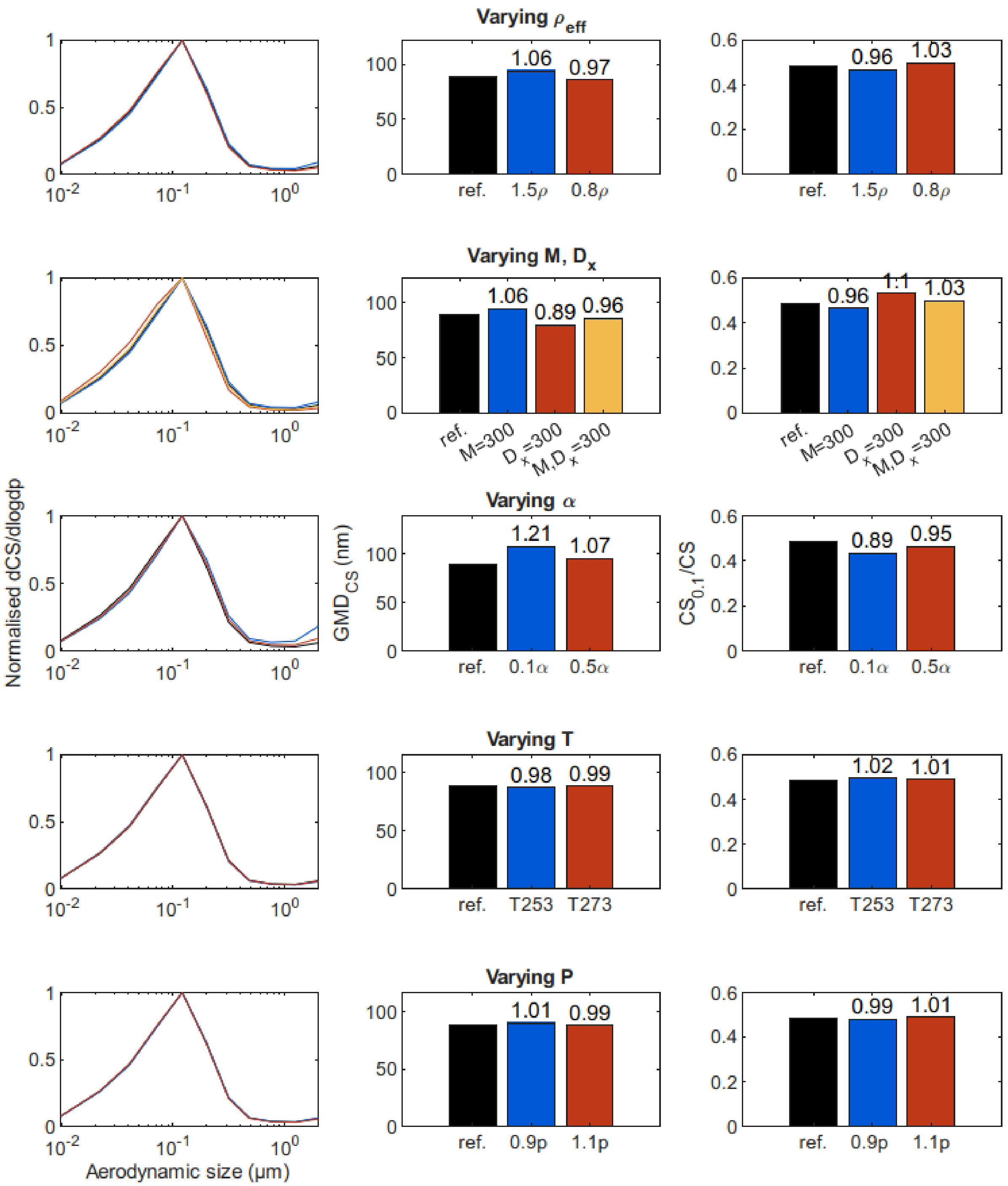


**Figure S10: The effect of varying input parameters of the calculation ($\rho_{eff}$, $\alpha$, $M_{vap}$, $D_{x,vap}$, $T$, $P$) on $GMD_{CS}$, $CS_{0.1}/CS_{2.5}$ and normalised CS size distribution at the studied location of Highway (Tampere). 1.5$\rho$ and 0.8$\rho$ indicate $\rho_{eff}$ of 1.5 and 0.8 g/cm$^3$, respectively. M = 300, $D_x$ = 300 indicate $M_{vap}$ of 300 g/mol, $D_{x,vap}$ of 300 cm$^3$, respectively (M,$D_x$ = 300 indicates both). 0.1$\alpha$ and 0.5$\alpha$ indicate $\alpha$ of 0.1 and 0.5, respectively. T253, T273, 0.9p and 1.1p indicate temperatures of 253 K and 273 K, and ambient pressure of 0.9 atm and 1.1 atm. The value on the bar plot shows the difference to default input parameter values (ref.)**

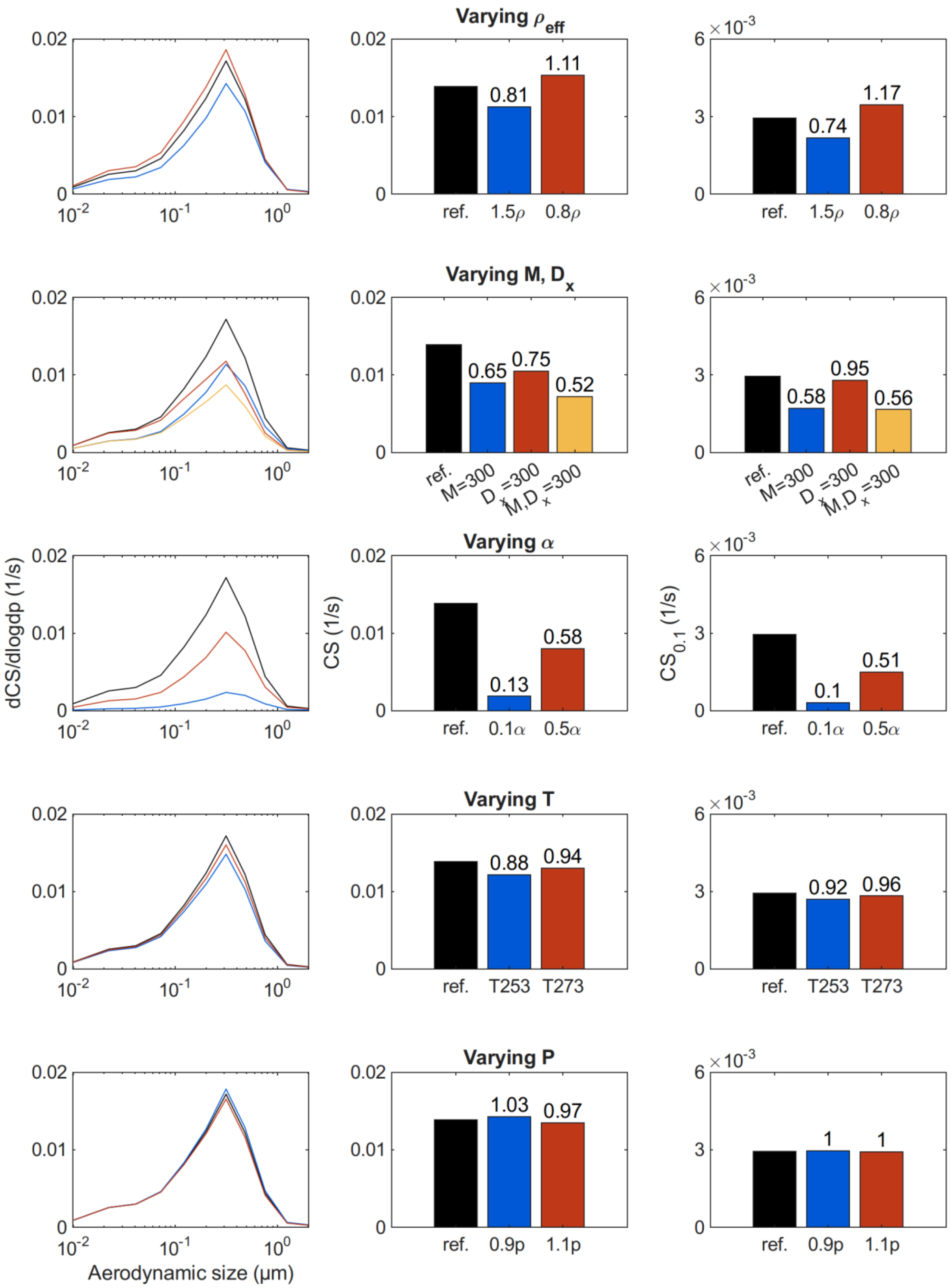


**Figure S11: The effect of varying input parameters of the calculation ($\rho_{eff}$, $\alpha$, $M_{vap}$, $D_{x,vap}$, $T$, $P$) on CS, $CS_{0.1}$ and CS size distribution at the studied location of Airport (Düsseldorf). 1.5$\rho$ and 0.8$\rho$ indicate $\rho_{eff}$ of 1.5 and 0.8 g/cm$^3$, respectively. M = 300, $D_x$ = 300 indicate $M_{vap}$ of 300 g/mol, $D_{x,vap}$ of 300 cm$^3$, respectively (M,$D_x$ = 300 indicates both). 0.1$\alpha$ and 0.5$\alpha$ indicate $\alpha$ of 0.1 and 0.5, respectively. T253, T273, 0.9p and 1.1p indicate temperatures of 253 K and 273 K, and ambient pressure of 0.9 atm and 1.1 atm. The value on the bar plot shows the difference to default input parameter values (ref.)**

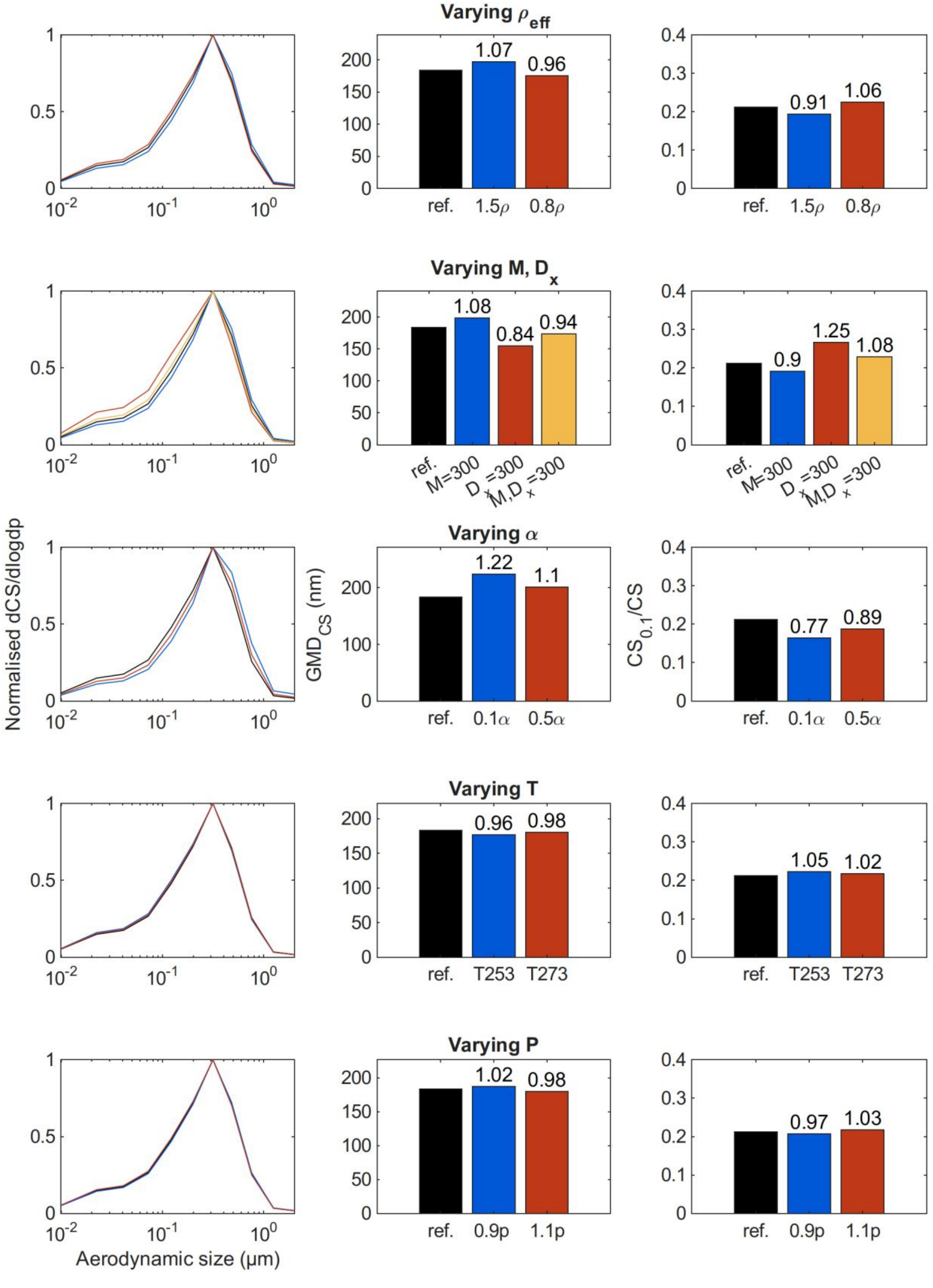


**Figure S12: The effect of varying input parameters of the calculation ($\rho_{eff}$, $\alpha$, $M_{vap}$, $D_{x,vap}$, $T$, $P$) on $GMD_{CS}$, $CS_{0.1}/CS_{2.5}$ and normalised CS size distribution at the studied location of Airport (Düsseldorf). 1.5$\rho$ and 0.8$\rho$ indicate $\rho_{eff}$ of 1.5 and 0.8 g/cm$^3$, respectively. M = 300, $D_x$ = 300 indicate $M_{vap}$ of 300 g/mol, $D_{x,vap}$ of 300 cm$^3$, respectively (M,$D_x$ = 300 indicates both). 0.1$\alpha$ and 0.5$\alpha$ indicate $\alpha$ of 0.1 and 0.5, respectively. T253, T273, 0.9p and 1.1p indicate temperatures of 253 K and 273 K, and ambient pressure of 0.9 atm and 1.1 atm. The value on the bar plot shows the difference to default input parameter values (ref.)**

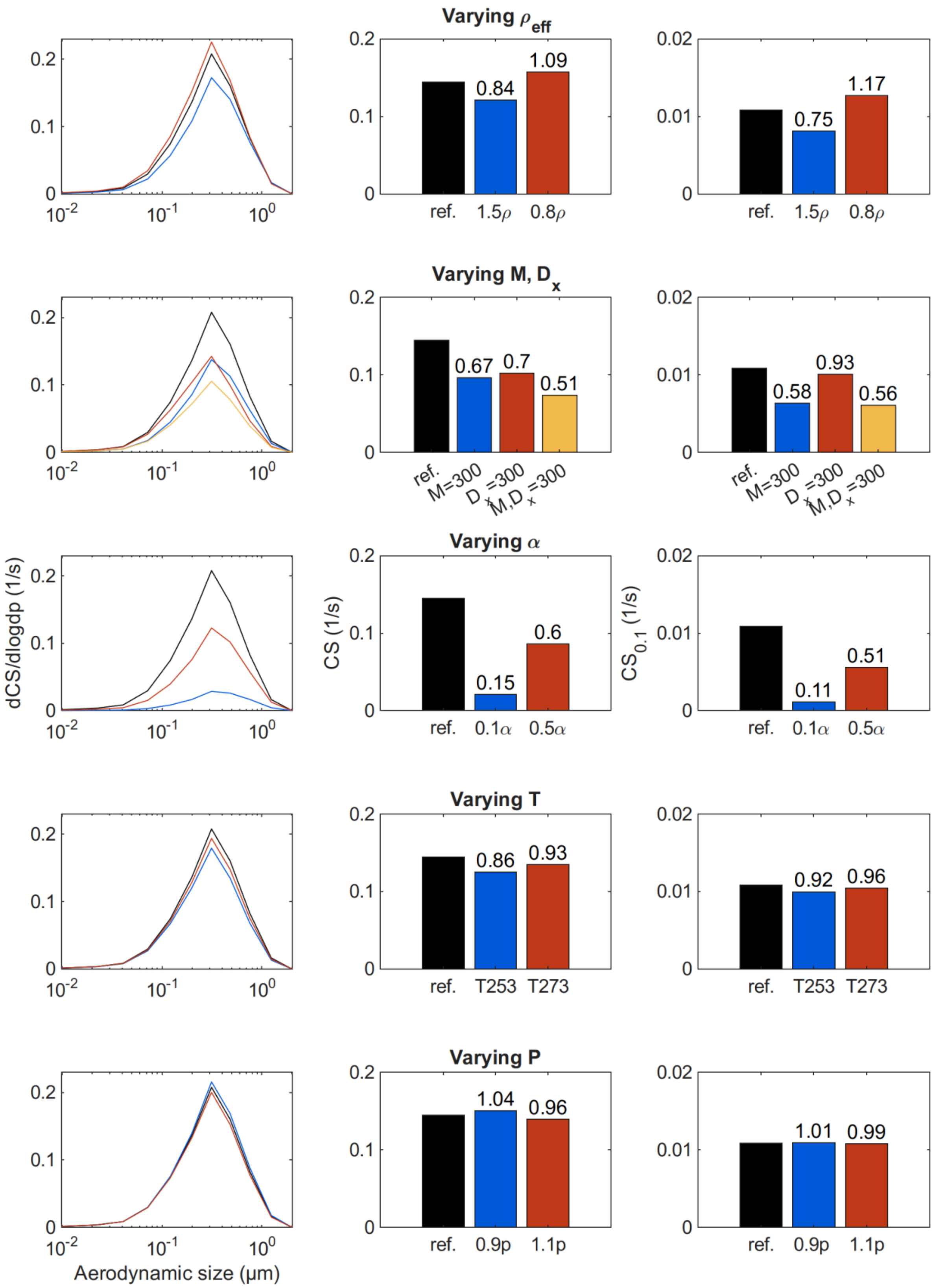


**Figure S13: The effect of varying input parameters of the calculation ($\rho_{eff}$, $\alpha$, $M_{vap}$, $D_{x,vap}$, $T$, $P$) on CS, $CS_{0.1}$ and CS size distribution at the studied location of Urban (Delhi-NCR). 1.5ρ and 0.8ρ indicate $\rho_{eff}$ of 1.5 and 0.8 g/cm$^3$, respectively. M = 300, $D_x$ = 300 indicate $M_{vap}$ of 300 g/mol, $D_{x,vap}$ of 300 cm$^3$, respectively (M,$D_x$ = 300 indicates both). 0.1α and 0.5α indicate α of 0.1 and 0.5, respectively. T253, T273, 0.9p and 1.1p indicate temperatures of 253 K and 273 K, and ambient pressure of 0.9 atm and 1.1 atm. The value on the bar plot shows the difference to default input parameter values (ref.)**

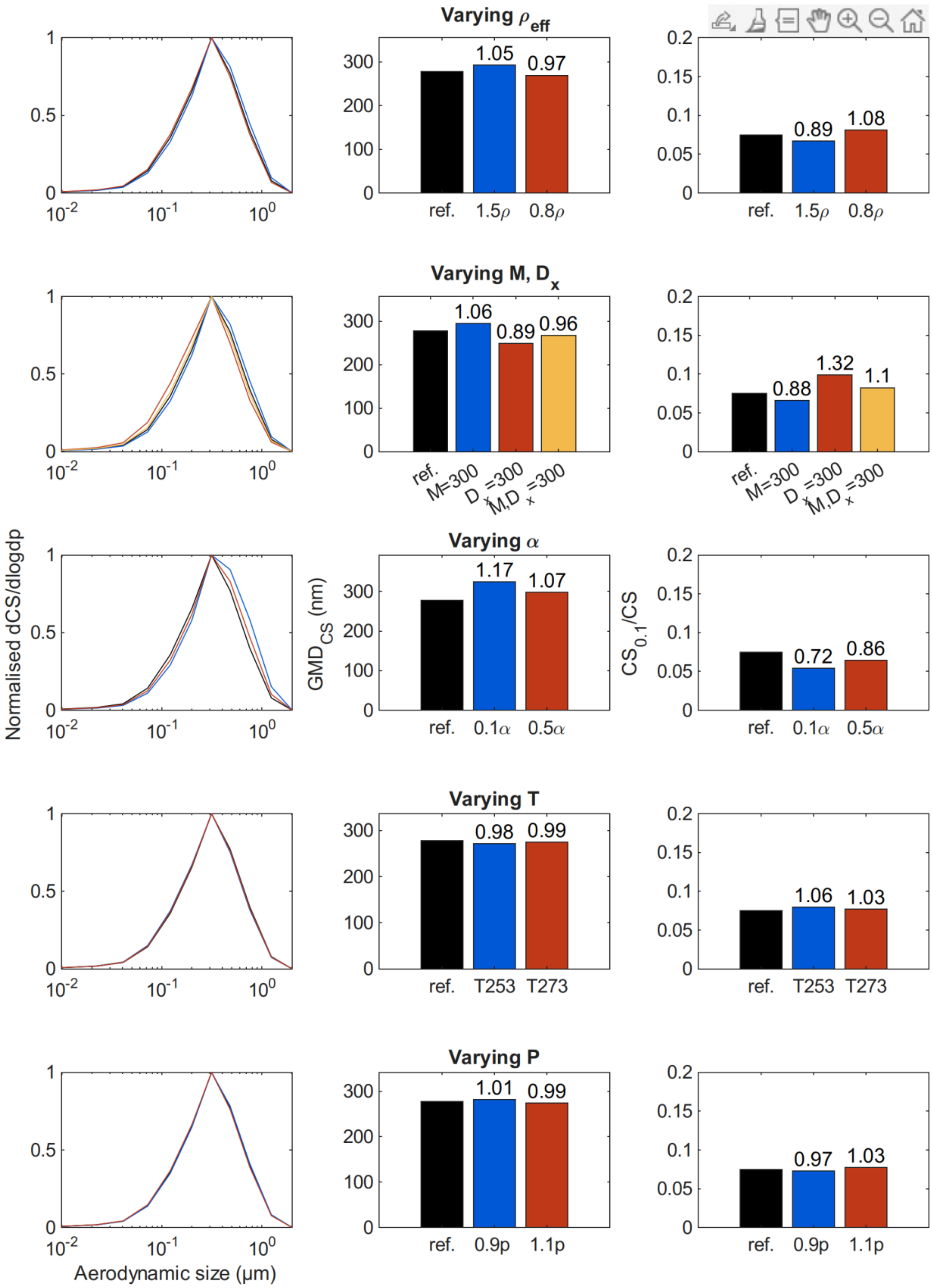


**Figure S14: The effect of varying input parameters of the calculation ($\rho_{eff}$, $\alpha$, $M_{vap}$, $D_{x,vap}$, $T$, $P$) on $GMD_{CS}$, $CS_{0.1}/CS_{2.5}$ and normalised CS size distribution at the studied location of Urban (Delhi-NCR). 1.5$\rho$ and 0.8$\rho$ indicate $\rho_{eff}$ of 1.5 and 0.8 g/cm$^3$, respectively. M = 300, $D_x$ = 300 indicate $M_{vap}$ of 300 g/mol, $D_{x,vap}$ of 300 cm$^3$, respectively (M,$D_x$ = 300 indicates both). 0.1$\alpha$ and 0.5$\alpha$ indicate $\alpha$ of 0.1 and 0.5, respectively. T253, T273, 0.9p and 1.1p indicate temperatures of 253 K and 273 K, and ambient pressure of 0.9 atm and 1.1 atm. The value on the bar plot shows the difference to default input parameter values (ref.)**

## The observation range of the CS size distributions

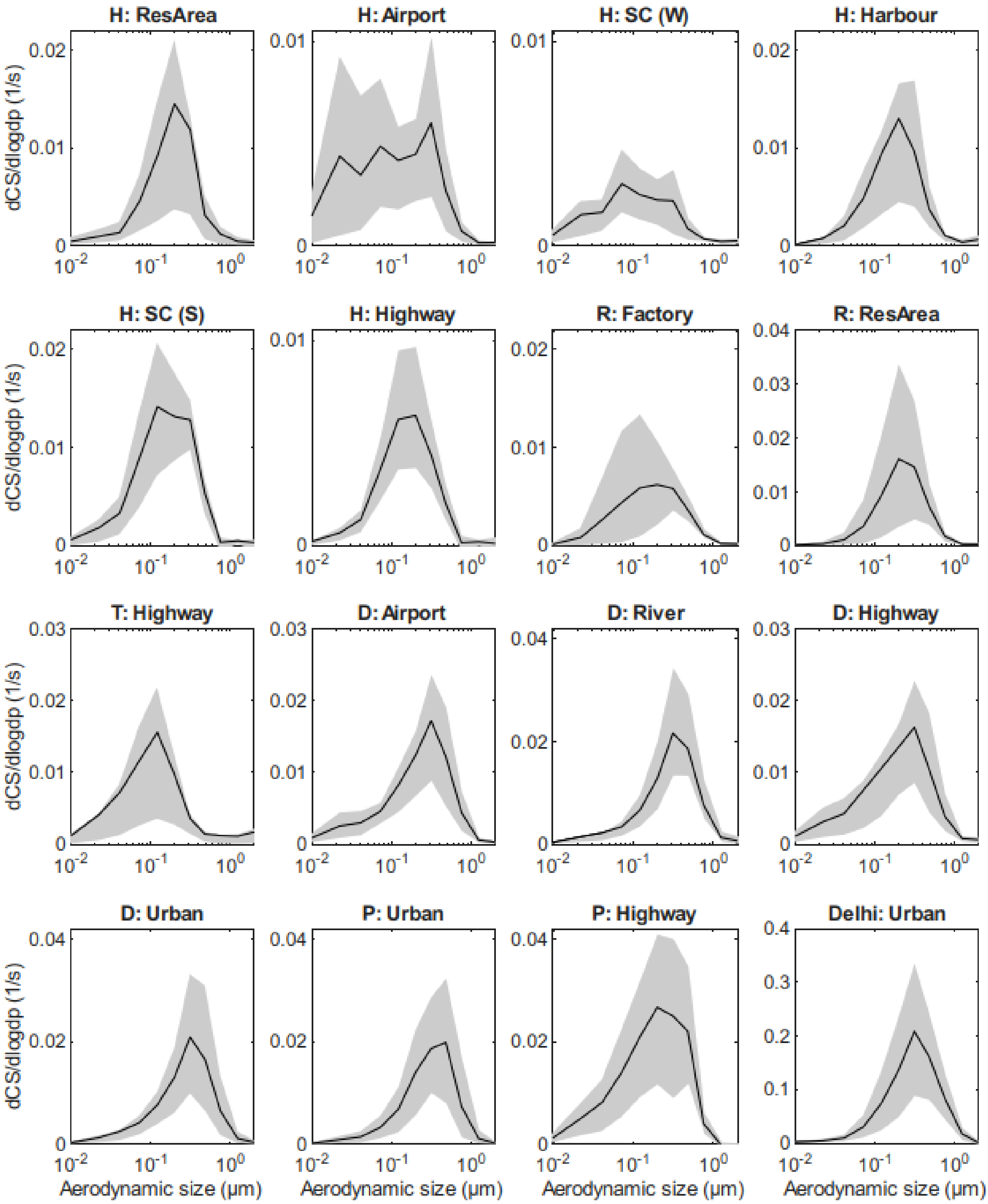


**Figure S15: The 15th and 85th percentiles (shaded) of the measured CS size distributions together with the average (solid line) at the studied locations. H, R, T, D, P and Delhi indicate Helsinki, Raahe, Tampere, Düsseldorf, Prague and Delhi-NCR, respectively, whereas SC and HW indicate, street canyon and highway. Urban indicates an urban traffic site and ResArea a residential area.**

**CS attributable to ultrafine particles ($CS_{0.1}$)**

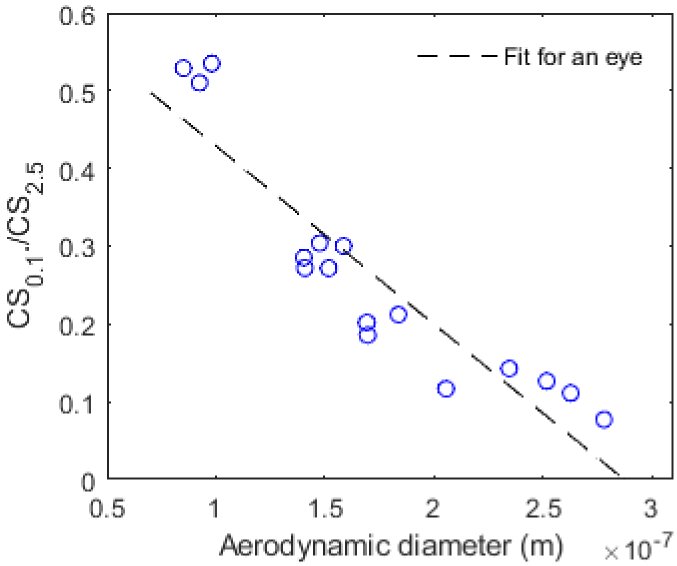


**Figure S16: The connection between CS attributable to ultrafine particles ($CS_{0.1}$) and total CS (of particles smaller than 2.5, $CS_{2.5}$) as a function of GMD size of CS size distribution in the studied environments.**

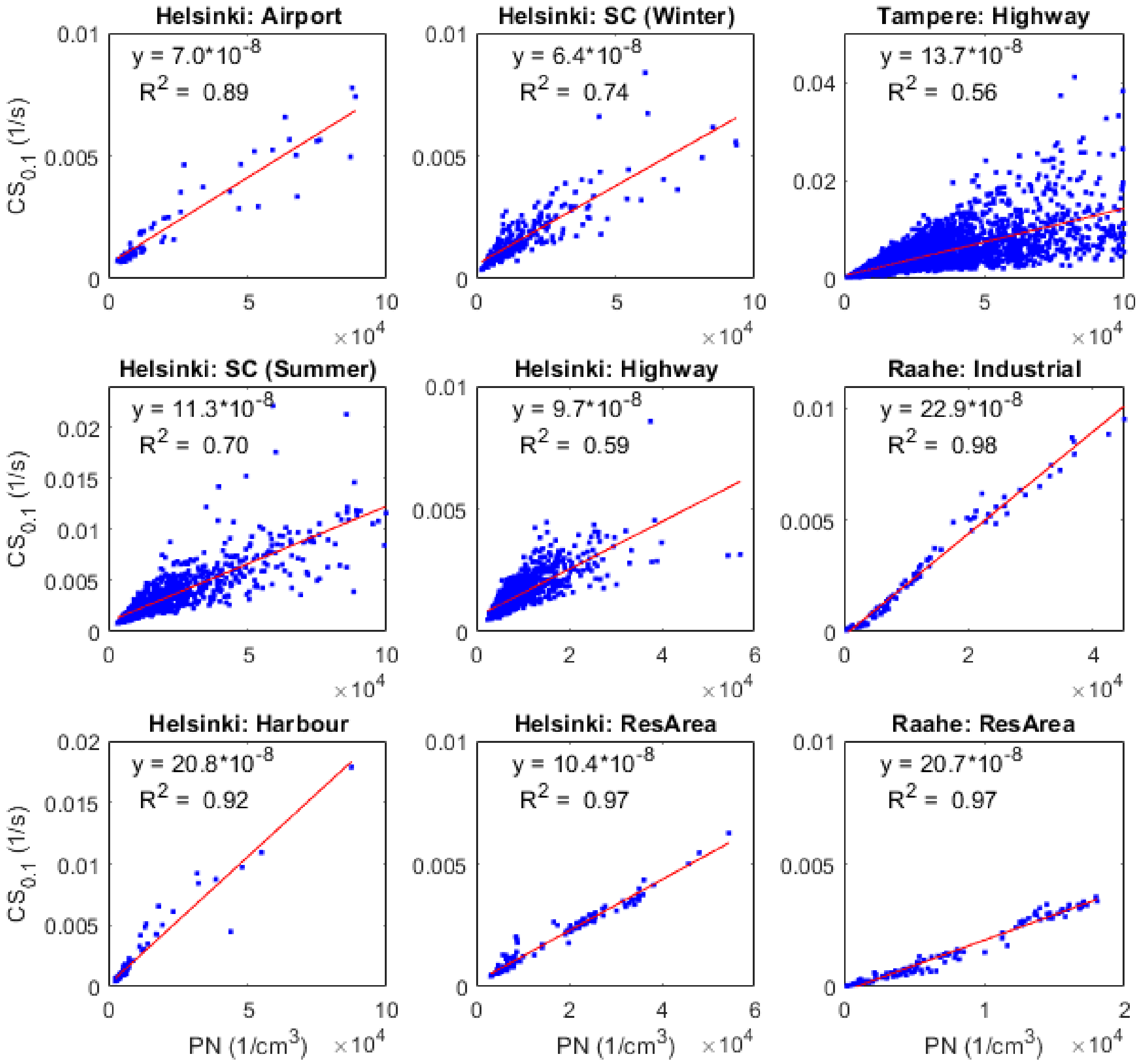


**Figure S17: Linear fits between CS attributable to ultrafine particles ($CS_{0.1}$) and PN concentration in the studied environments in Finland. Here, outliers of PN > $10^5$ 1/cm$^3$ were neglected.**

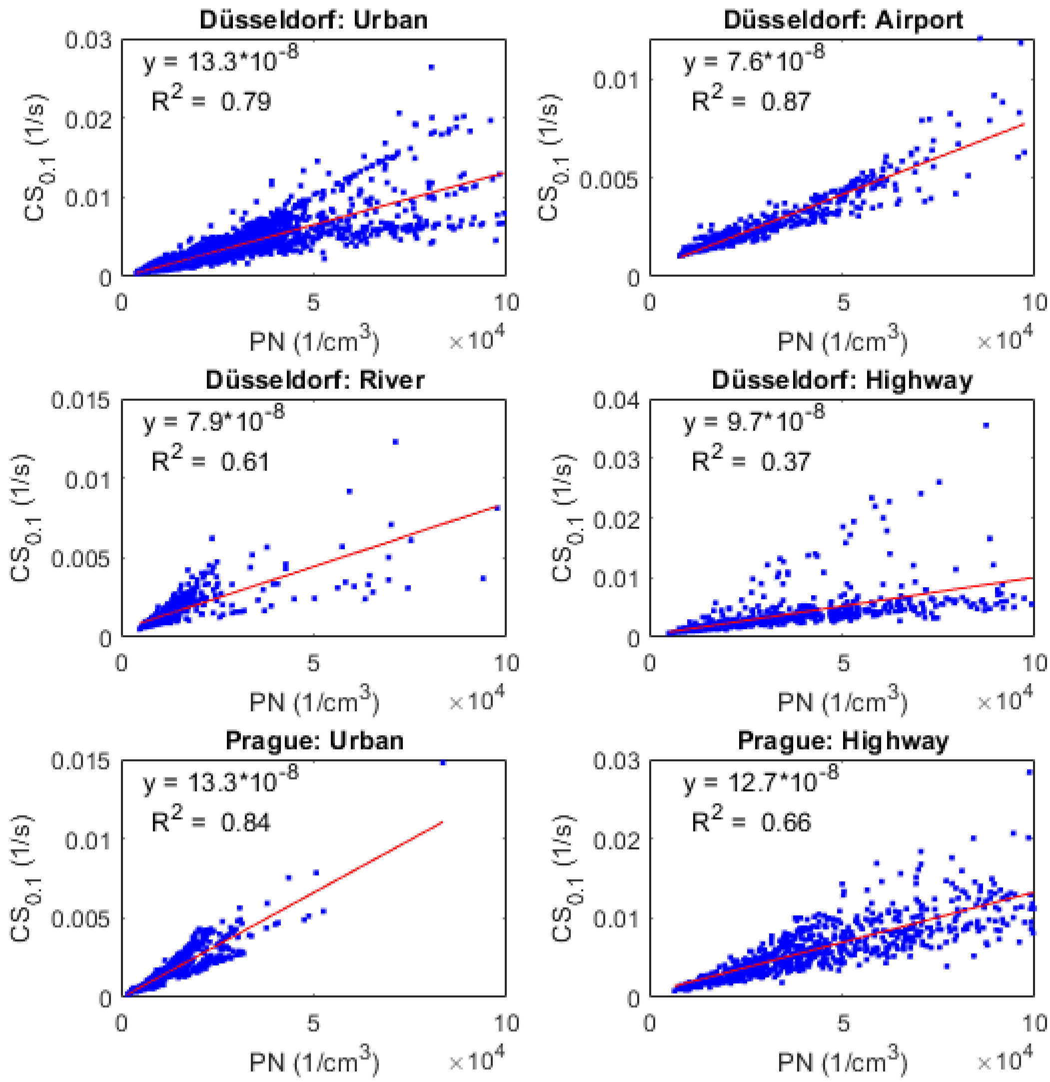


**Figure S18: Linear fits between CS attributable to ultrafine particles ($CS_{0.1}$) and PN concentration in the studied environments in Central Europe. Here, outliers of PN > $10^5$ 1/cm$^3$ were neglected.**

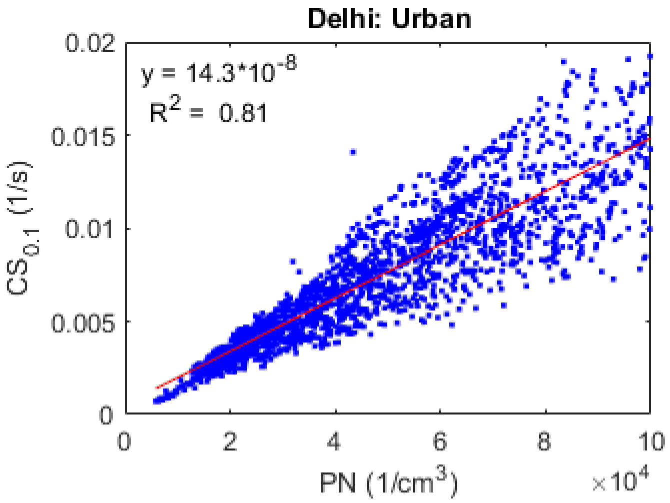


**Figure S19: Linear fit between CS attributable to ultrafine particles ($CS_{0.1}$) and PN concentration in Delhi-NCR. Here, PN > $10^5$ 1/cm$^3$ results were neglected to keep the same criteria as in Fig. S10-11.**

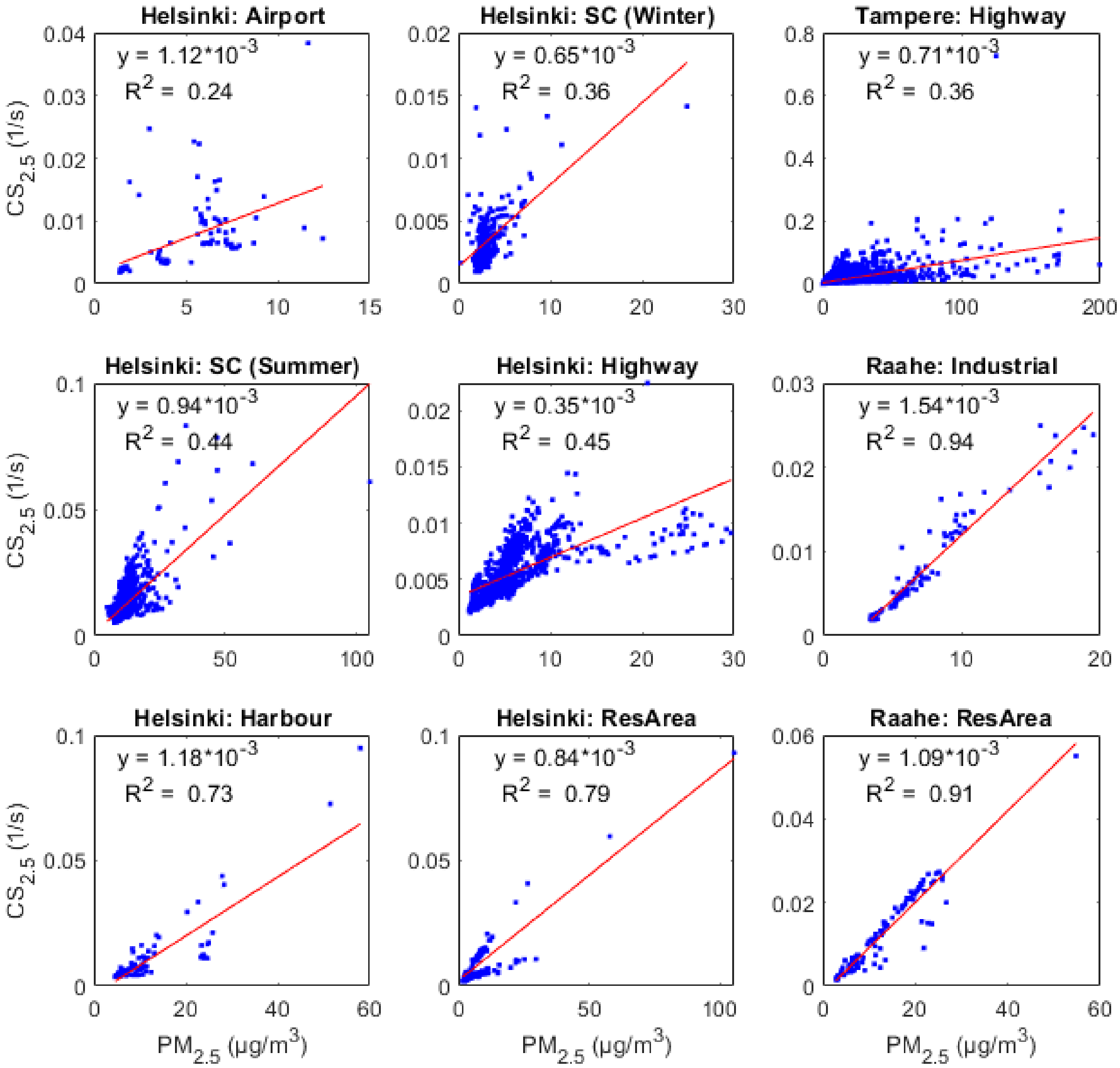


**Figure S20: Linear fits between CS particles smaller than 2.5 µm ($CS_{2.5}$) and $PM_{2.5}$ in the studied environments in Finland. Here, outliers of $PM_{2.5}$ > 200 µg/m$^3$ were neglected.**

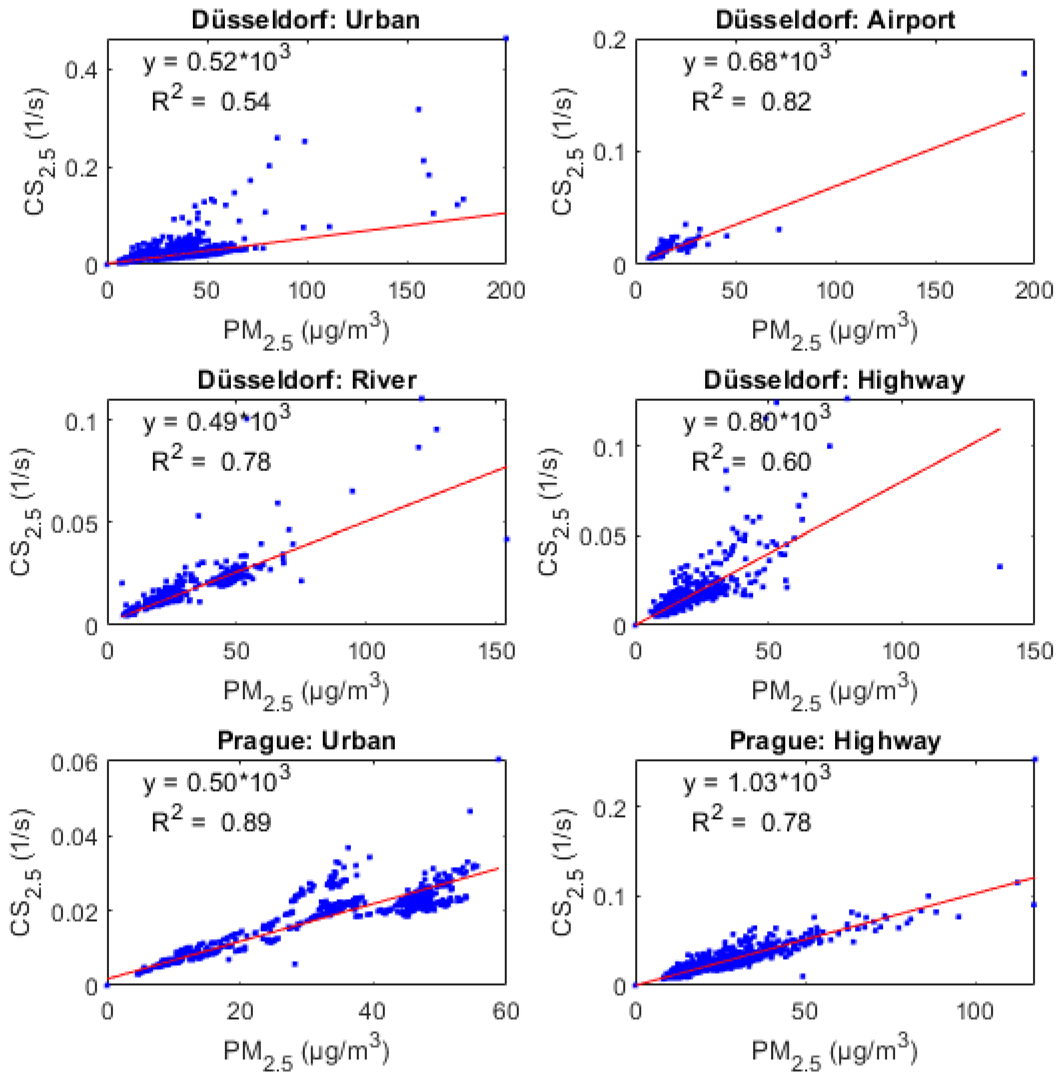


**Figure S21: Linear fits between CS particles smaller than 2.5 µm ($CS_{2.5}$) and $PM_{2.5}$ in the studied environments in Central Europe. Here, outliers of $PM_{2.5}$ > 200 µg/m³ were neglected.**

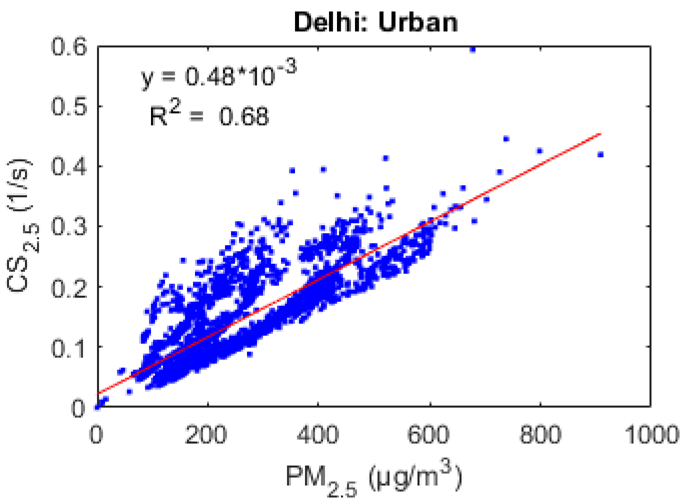


**Figure S22: Linear fit between CS particles smaller than 2.5 µm ($CS_{2.5}$) and $PM_{2.5}$ in Delhi-NCR. Here, outliers of $PM_{2.5}$ > 1000 µg/m³ were neglected.**